Moments in nuclear resonant inelastic x-ray scattering and their applications

Michael Y. Hu,[1,*] Thomas S. Toellner,[1] Nicolas Dauphas,[2] E. Ercan Alp,[1] and Jiyong Zhao[1]
[1]*Advanced Photon Source, Argonne National Laboratory, Argonne, Illinois 60439*
[2]*Origins Laboratory, Department of the Geophysical Sciences and Enrico Fermi Institute, The University of Chicago, 5734 South Ellis Avenue, Chicago, Illinois 60637, USA*

(Received 1 September 2012; revised manuscript received 10 December 2012; published 8 February 2013)

Sum rules of the moments of the nuclear resonant inelastic x-ray scattering (NRIXS) spectrum provide means of data analysis and information on atomic dynamics. We extend existing work by calculating the third and fourth moment beyond the harmonic approximation and show that NRIXS can provide a direct measurement of the anharmonic terms in lattice potentials. Projected partial phonon density of states (ppDOS) extracted from measured spectra provide vibrational mode-specific information on lattice dynamics. Furthermore, unique contributions to thermodynamic properties can be defined and calculated as the moments and other weighted integrals of ppDOS. A summary of some of these thermodynamic quantities is given. The directional dependence of NRIXS and its effects are emphasized. We derive explicit relationships between the moments of phonon excitation probability function and those of ppDOS. The comparison between the two sets of moments provides a consistency check and insights to the lattice dynamics of the system under study.

DOI: 10.1103/PhysRevB.87.064301 PACS number(s): 61.05.cc, 63.20.−e

I. INTRODUCTION

Nuclear resonant inelastic x-ray scattering (NRIXS) is a synchrotron-radiation-based method that finds a wide range of applications in condensed matter physics,[1] materials science, high-pressure research,[2] geosciences,[3] and biophysics.[4] A recent development is its application in the field of geochemistry and cosmochemistry concerning isotope fractionation.[5] Through thermodynamic arguments, one can relate the equilibrium isotope fractionation factor to mean kinetic energy[6] or mean force constant.[7] This emphasizes the importance of moments derived from NRIXS measurements. In materials research, e.g., of nanoparticles,[8] it is of critical importance to understand atomic dynamics and lattice thermodynamic properties, some of which can be derived from moments of an NRIXS measurement.

NRIXS is an incoherent inelastic process. The experimental setups and procedures have been described in almost all publications where this technique is used, and excellent explanations can be found in the above mentioned references. In an NRIXS experiment, one measures the number of nuclear resonant absorption events as a function of energy transfer from an incident x-ray beam to the sample under study. Thus nuclear resonant isotopes are employed as probes to lattice vibration properties. Vastly disparate energy scales involved in nuclear excitations (many kilo-electron-volts here) and atomic lattice excitations (tens of milli-electron-volts) implicate the decoupling of these two processes. NRIXS can be described as nuclear resonant excitation plus phonon annihilation or creation. As a result, on the scale of the energies of phonons, the energy of nuclear resonant absorption is modified only through atomic motions in a sample. This is reflected in the cross section of nuclear resonant absorption from suitable isotopes embedded in an interacting collection of atoms. It can be factorized into the properties of nuclear resonant absorption by an isolated nucleus and the dynamical property of the scattering system. Van Hove[9] and Visscher[10] studied scattering from a collection of interacting particles. For NRIXS, the cross section per nucleus is given by[11,12]

$$\sigma(\mathbf{k},E) = \frac{\pi}{2}\sigma_0\Gamma\, S(\mathbf{k},E)\,, \tag{1}$$

where $E = E_{\rm in} - E_0$ is the energy difference between incident x-ray and the nuclear resonance and is of the order of tens to hundreds of milli-electron-volts; $\hbar\mathbf{k}$ is the incident photon momentum and for all practical purposes is a constant so that $\hbar kc = E_0$ to a very good approximation, σ_0 is the maximum nuclear resonant absorption cross section, Γ is the natural linewidth of the excited nuclear level, and $S(\mathbf{k},E)$ is a dynamical function characterizing the lattice vibrations of the sample. The measured spectrum is proportional to the sum of the cross sections from all resonant nuclei, whose number is $\tilde{N}$, which may be smaller than N, the number of all atoms in the sample.

The dynamical function above can be treated as a Fourier transform of the particle autocorrelation function of a many-body system,[11]

$$S(\mathbf{k},E) \equiv \frac{1}{2\pi\hbar}\int dt d\mathbf{r}\, e^{i(\mathbf{kr}-\frac{E}{\hbar}t)} G_a(\mathbf{r},t)\,, \tag{2}$$

where

$$G_a(\mathbf{r},t) = \frac{1}{\tilde{N}}\left\langle \sum_\nu \int d\mathbf{r}'\delta[\mathbf{r}+\mathbf{r}_\nu(0)-\mathbf{r}']\,\delta[\mathbf{r}'-\mathbf{r}_\nu(t)]\right\rangle_T, \tag{3}$$

and ν enumerates resonant nuclei. $\mathbf{r}_\nu$ is the position of the νth nucleus. The statistical average at a given temperature T is indicated by $\langle\cdots\rangle_T$. The expression in Eq. (2) is similar to the dynamic structure factor $S(\mathbf{q},\omega)$, a function of energy and momentum transfer defined by the same equation but with the particle pair correlation function instead. Phonon dispersions can be determined by measuring the dynamic structure factor with coherent inelastic neutron scattering[13] and inelastic x-ray scattering.[14] In contrast, the function $S(\mathbf{k},E)$ obtained from NRIXS is a function of energy transfer to and from lattice vibrations and the incident x-ray momentum

instead of momentum transfer. It can be interpreted as the phonon excitation probability density and is closely related to phonon density of states.[12]

Sum rules of the moments of $S(\mathbf{k},E)$ can be related to dynamical properties of the resonant nuclei in a sample.[15] In Sec. II, we extend existing results to derive the third and fourth moments beyond the quasiharmonic lattice model. The ppDOS extracted from measured spectra provides vibrational mode specific information on the lattice dynamics of the samples studied. Its moments and other weighted integrals are related to the resonant nucleus sublattice contributions to thermodynamic properties. A summary of these quantities derivable from an NRIXS measurement is given in Sec. III. Then, in Sec. IV, we present relations between the moments of $S(\mathbf{k},E)$ and those of ppDOS in the context of a quasiharmonic lattice model. The case of multiple nonequivalent sites is discussed in Sec. V. A recent study of several minerals is presented as examples in Sec. VI. Uncertainty estimations of the moments derived from an NRIXS measurement are given in Sec. VII followed by a brief summary. Some of the details of derivations are shown in the appendices at the end. Calculation of the central moments of $S(\mathbf{k},E)$ is shown in Appendix A. Appendix B summarizes the derivation of ppDOS from measured spectrum. Appendix C details how the $S(\mathbf{k},E)$ moments can be expressed in terms of the moments of ppDOS.

II. MOMENTS OF S(E)

Sum rules of the Mössbauer energy spectrum were studied soon after the discovery of the Mössbauer effect to help understand the effect and reveal its quantum nature.[16] The first and second moments were studied in detail, as well as laying out the general formulas. With the discovery of NRIXS, the sum rules were extended up to the fourth moment in the context of the harmonic approximation.[15] In particular, the third moment of a measured spectrum was related to a mean force constant. Since then, the results have also been presented in many different contexts.[17–21] The sum rules are based on a sudden momentum transfer to a constituent of a complex bound system by emission, absorption, or scattering. Here, the process is the absorption of a photon by a nucleus bound in an atomic lattice. Nuclear resonant scattering with current synchrotron sources happens in a weak scattering regime. The probability of finding two nuclei in excited states simultaneously is practically zero. Thus we can sum over all nuclei the transition matrix elements due to a sudden momentum transfer.

Our focus is on the physical interpretation of the moments, that is, the relations of these moments to atomic dynamical properties. In particular, we will calculate the third and fourth moments independent of the quasiharmonic lattice model. Here and throughout the following discussions, we use $\tilde{m}$ to represent the mass of a resonance nucleus. It turns out that the central moments of $S(\mathbf{k},E)$ with respect to the nuclear recoil energy $E_R = (\hbar k)^2/2\tilde{m}$ have more straightforward interpretations. To that effect, we define central moments as

$$R_l(\mathbf{k}) \equiv \int_{-\infty}^{+\infty} (E - E_R)^l \, S(\mathbf{k},E)\, dE\,. \tag{4}$$

It has been established that the first few low-order moments are

$$R_0 = 1\,, \tag{5}$$

$$R_1 = 0\,, \tag{6}$$

$$R_2 = 4\,E_R\,T_{\hat{\mathbf{k}}}\,, \tag{7}$$

$$R_3 = \frac{\hbar^2 E_R}{\tilde{m}} \left\langle \frac{\partial^2 V}{\partial z^2} \right\rangle . \tag{8}$$

Their derivations can be found in Appendix A. The first equation expresses the normalization of $S(\mathbf{k},E)$. The vanishing first central moment provides a means to normalize the measured spectrum to obtain $S(\mathbf{k},E)$, because the elastic peak in a measured spectrum has different normalization than the rest of the spectrum.[15,22]

In the above equations, $\hat{\mathbf{k}} = \mathbf{k}/k$, is the unit vector along the incident photon direction. The coordinate along this direction is z. One very important feature of NRIXS is its directional dependence.[23] As discussed in the introduction, the energy of nuclear resonant absorption is modified through atomic motions. It is the atomic motion along the incident photon direction specifically. To emphasize this characteristics and be concise, we shall use "projected" as a qualifier to describe many of the quantities derived from an NRIXS measurement, as in the often used term, projected phonon DOS.[23] The reason for using "projected" is because $\mathbf{k}$ appears in the scalar products with phonon polarization vectors.

The second moment is related to $T_{\hat{\mathbf{k}}}$, the mean kinetic energy from atomic motion along $\hat{\mathbf{k}}$ direction. For an isotropic sample, it is $1/3$ of the mean kinetic energy per nucleus. In a harmonic model, by the virial theorem, it is $1/6$ of the internal energy per atom.

For the third moment, the brackets represent thermodynamic and quantum mechanical expectation value, and V is the potential part of the lattice Hamiltonian

$$H = T + V = \sum_{\mu} \frac{p_\mu^2}{2m_\mu} + \frac{1}{2}\sum_{\mu\mu'} V(\mathbf{r}_\mu, \mathbf{r}_{\mu'})\,. \tag{9}$$

In the quasiharmonic approximation, effective potentials are quadratic, thus the third moment is proportional to the mean force constant along the photon direction $K_{\hat{\mathbf{k}}}$,

$$R_3 = \frac{\hbar^2 E_R}{\tilde{m}}\, K_{\hat{\mathbf{k}}}\,. \tag{10}$$

Beyond the harmonic model, considering an anharmonic potential up to the quartic term, we have

$$\frac{\partial^2 V}{\partial z^2} = K_{\hat{\mathbf{k}}} + A_{\hat{\mathbf{k}}} z + \frac{B_{\hat{\mathbf{k}}}}{2} z^2, \tag{11}$$

with

$$K_{\hat{\mathbf{k}}} = \left.\frac{\partial^2 V}{\partial z^2}\right|_{\text{eq}}, \tag{12}$$

$$A_{\hat{\mathbf{k}}} = \left.\frac{\partial^3 V}{\partial z^3}\right|_{\text{eq}}, \tag{13}$$

$$B_{\hat{\mathbf{k}}} = \left.\frac{\partial^4 V}{\partial z^4}\right|_{\text{eq}}, \tag{14}$$

which are evaluated at the equilibrium atomic positions. They are, respectively, the directional force constant, the third- and fourth-order coupling parameters along $\hat{\mathbf{k}}$ direction. For a sample at equilibrium, the mean displacement in any direction is zero; thus we can neglect the A term to yield

$$R_3 = \frac{\hbar^2 E_R}{\tilde{m}} \left(K_{\hat{\mathbf{k}}} + \frac{B_{\hat{\mathbf{k}}}}{2} \langle z^2 \rangle \right), \tag{15}$$

where $\langle z^2 \rangle$ is the atomic mean square displacement in $\hat{\mathbf{k}}$ direction, which can be calculated from the directional Lamb-Mössbauer factor, or f factor, through Eq. (B15). This f factor can be determined from a measured NRIXS spectrum, as shown later in this section. The mean square displacement varies with either temperature or pressure, or both. If one plots R_3 versus $\langle z^2 \rangle$, the slope at each point is the coefficient $B_{\hat{\mathbf{k}}}$ of the quartic term in the lattice potential and the y intercept is the mean force constant at the corresponding condition. This indicates a way of direct measurement of the anharmonic corrections to a lattice potential.

For the fourth moment, we find the following expression, whose detailed derivation can be found in Appendix A,

$$R_4(\mathbf{k}) = \frac{2E_R}{\tilde{m}} \left[\left\langle \hbar^2 \left(\frac{\partial V}{\partial z} \right)^2 \right\rangle + \frac{2E_R}{\tilde{m}} \langle p_z^4 \rangle - \frac{\hbar^2 E_0}{\tilde{m} c} \left\langle p_z \frac{\partial^2 V}{\partial z^2} + \frac{\partial^2 V}{\partial z^2} p_z \right\rangle \right]. \tag{16}$$

The first term is proportional to the mean square force along $\hat{\mathbf{k}}$ direction, which can also be expressed as

$$\frac{2E_R}{\tilde{m}} \hbar^2 \left\langle \left(\frac{\partial V}{\partial z} \right)^2 \right\rangle = 4E_R \sum_i g_i \langle i | \frac{p_z^2}{2\tilde{m}} | i \rangle \sum_f (E_f - E_i)^2 . \tag{17}$$

It can be shown that the last term in the above expression of $R_4(\mathbf{k})$ contains a contribution stemming from the cubic coupling constant $A_{\hat{\mathbf{k}}}$. In the quasiharmonic approximation, this term vanishes and $R_4(\mathbf{k})$ reduces to the result given previously.[15]

The above equations can be used to calculate these moments, given any specific model of lattice potentials, and the results can then be compared to the moments of a measured spectrum. This may be used to restrict and adjust models of lattice potentials.

In calculating $S(\mathbf{k}, E)$ from a measured spectrum $I(E)$, special care has to be taken due to a unique effect mentioned earlier. Because of the strong coherent forward scattering when incident x-ray energy coincides with the nuclear resonant energy E_0, a great number of nuclear decay events escape detection in a typical NRIXS setup; thus the elastic peak count is much smaller than what it would be if the same fraction of decay events were included as for other parts of an NRIXS spectrum. A model for this effect was discussed in a study of NRIXS.[24] As a result, $I(E)$ has a different normalization factor near the zero energy difference. If we remove the elastic peak from $I(E)$, then the rest should normalize to $1 - f$, where f is the recoil free fraction, also called the Lamb-Mössbauer factor. However, this f factor is not often known, or its value may have large uncertainty. The difficulty is dealt with in the following way. We have an internal constraint, which is that the first moment is equal to the recoil energy E_R, whose value is known quite accurately. This is reflected in Eq. (6). If the experimental resolution function is sufficiently symmetric, then the elastic peak, which is the resolution function, will not contribute to the first moment. This allows us to renormalize the peak-removed spectrum so that its first moment equals the recoil energy for the isotope used. Once it is normalized, we can immediately infer the f factor from its zeroth moment. Now, we add back the elastic peak to this normalized peak-removed spectrum to obtain the normalization-corrected spectrum

$$I_c(E) = \frac{1}{A} I'(E) + f\, R(E) , \tag{18}$$

where $R(E)$ is the experimentally measured resolution function normalized to unity.

Next, we shall consider the effect on moment calculations due to a resolution function with a finite width. Moments in the presence of a finite resolution function have been considered previously.[20,25] Here, we shall discuss the central moments, which have simpler expressions. The above obtained spectrum $I_c(E)$ is a convolution of phonon excitation probability density with the resolution function

$$I_c(E) = \int S(E') R(E - E')\, dE' , \tag{19}$$

where the photon momentum dependence is ignored to simplify the expression. One can show that the central moments of $I_c(E)$ and $S(E)$, and the regular moments of $R(E)$ satisfy the following relation:

$$I_n = \sum_{k=0}^{n} C_n^k\, R_k\, m_{n-k} , \tag{20}$$

where

$$I_n = \int (E - E_R)^n\, I_c(E)\, dE , \tag{21}$$

$$m_j = \int E^j\, R(E)\, dE , \tag{22}$$

and C_n^k are the binomial coefficients. Since both $S(E)$ and $R(E)$ are normalized to unity and $R_1 = 0$, for the first a few terms, we have

$$I_1 = m_1 , \tag{23}$$

$$I_2 = R_2 + m_2 , \tag{24}$$

$$I_3 = R_3 + 3R_2 m_1 + m_3 , \tag{25}$$

$$I_4 = R_4 + 4R_3 m_1 + 6R_2 m_2 + m_4 . \tag{26}$$

For a sufficiently symmetric resolution function, all the odd moments m_{2k+1} are small. The second moment m_2 is on the order of resolution width squared. The above equations indicate that finite experimental resolution may require corrections in calculating moments from a measured spectrum. As an example, let us calculate these corrections in a case that involves a measurement on bcc iron metal. In this example, the resolution function has a width (FWHM) of 0.9 meV and the results are listed in Table I. Here, the corrections are small, demonstrating a sufficiently narrow and symmetric

TABLE I. Corrections to central moments due to a finite resolution function, with a width (FWHM) of 0.9 meV. The spectrum was taken on a sample of bcc iron metal.

order n	m_n (meV^n)	I_n (meV^n)	R_n (meV^n)	corrections
1	−0.019	−0.019	0	0
2	1.053	110.63	109.58	−0.95%
3	0.0032	1590.4	1596.7	0.39%
4	32.16	131443	130840	−0.46%

resolution function for the purpose of studying moments in this case. This can be attributed to the small odd moments and relatively small even moments of the resolution function, and it should illustrate the need to select proper width and control the symmetry of a resolution function and recognize it as a possible source of errors in moment calculations otherwise.

III. DOS MOMENTS AND LATTICE THERMODYNAMICS

While moments of $S(\mathbf{k},E)$ give some averaged properties of atomic dynamics, the spectrum itself contains much more detailed information. A critical step in the development of NRIXS was the realization that phonon DOS could be derived from an NRIXS spectrum.[22] It is done in the context of the quasiharmonic lattice model. The derivation has been described many times before.[12,21,26,27] A brief reiteration of this derivation is given in Appendix B.

Projected partial phonon DOS characterizes the vibrational dynamics of a sublattice of resonant nuclei. Its detailed structure is related to the relevant vibrational modes, while the moments and weighted integrals provide atomic dynamics as well as macroscopic thermodynamic properties.

Let us define the moments of ppDOS as follows:

$$g_l(\mathbf{k}) \equiv \int_0^{+\infty} E^l\, \mathcal{D}(\mathbf{k},E)\, dE\,, \tag{27}$$

$$\tilde{g}_l(\mathbf{k}) \equiv \int_0^{+\infty} \frac{1}{2}\coth\left(\frac{\beta E}{2}\right) E^l\, \mathcal{D}(\mathbf{k},E)\, dE\,, \tag{28}$$

where $\tilde{g}_l$ are thermally averaged moments, for $\coth(\beta E/2) = 2\,n(E)+1$ and $n(E)$ being the phonon occupation number of energy level E. These are useful quantities since they carry information on thermal excitation, which allow temperature effects to be studied. Both definitions can be expressed in a unified fashion as shown in Kohn and Chumakov,[20] where $\tilde{g}_{-1}$ to g_2 were expressed. As mentioned in the above section, a unique feature of these moments and the related thermodynamic properties is that they are directional. This directional dependence can be revealed in NRIXS studies of anisotropic single crystals or textured samples.[23] Also as discussed before, we will call these thermodynamic quantities "projected," which shall be regarded as a shorthand for directional contributions. They are also called "partial," as only the resonant nucleus sublattice contributes.

Various thermodynamic quantities can be calculated from ppDOS derived from an NRIXS measurement.[28] Here, we list a few. First, let us consider a simple case where all resonant nuclei occupy equivalent sites in a crystal. The case for multiple nonequivalent sites will be discussed later in Sec. V.

The mean square displacement along the photon direction is given by

$$\langle z^2\rangle = \int \frac{\hbar^2}{\tilde{m}E}\left[n(E)+\frac{1}{2}\right]\mathcal{D}(\mathbf{k},E)\,dE = \frac{\hbar^2}{\tilde{m}}\tilde{g}_{-1}(\mathbf{k})\,. \tag{29}$$

This is related to the directional Lamb-Mössbauer factor, as expressed in Eq. (B15) of Appendix B.

The projected partial internal energy is given by

$$U_{\hat{k}} = \int E\left[n(E)+\frac{1}{2}\right]\mathcal{D}(\mathbf{k},E)\,dE = \tilde{g}_1(\mathbf{k})\,, \tag{30}$$

from which, by the virial theorem, the mean kinetic energy of resonant nucleus due to their thermal motions along the photon direction is given by

$$T_{\hat{k}} = \frac{1}{2}U_{\hat{k}} = \frac{1}{2}\tilde{g}_1(\mathbf{k})\,. \tag{31}$$

It can be shown that for an isotropic sample,

$$U_{\rm iso} = \int E\left[n(E)+\frac{1}{2}\right]g(E)\,dE = \frac{1}{3}\,U\,, \tag{32}$$

while for a powder sample,

$$U_{\rm pow} = \int |\epsilon(E)|^2\, E\left[n(E)+\frac{1}{2}\right]g(E)\,dE\,, \tag{33}$$

where $g(E)$ is the regular nonprojected partial phonon DOS, and $\epsilon(E)$ is the phonon polarization vector. The symbol U in Eq. (32) and others without any subscript in the following represent the thermodynamic quantities that are partial but not projected, just like their conventional counterparts expressed in the commonly defined phonon DOS. The difference between isotropic and powder samples is emphasized here; it stems from the different treatments of polarization vectors in each case, as shown in Appendix B.

The projected partial Helmholtz free energy is given by

$$F_{\hat{k}} = k_B T\int \ln\left(2\sinh\frac{\beta E}{2}\right)\mathcal{D}(\mathbf{k},E)\,dE\,. \tag{34}$$

Again, for an isotropic sample,

$$F_{\rm iso} = k_B T\int \ln\left(2\sinh\frac{\beta E}{2}\right)g(E)\,dE = \frac{1}{3}\,F\,, \tag{35}$$

while for a powder sample,

$$F_{\rm pow} = k_B T\int |\epsilon(E)|^2\,\ln\left(2\sinh\frac{\beta E}{2}\right)g(E)\,dE\,. \tag{36}$$

The projected partial vibrational entropy is given by

$$S_{\hat{k}} = k_B\int\left[\frac{\beta E}{2}\coth\left(\frac{\beta E}{2}\right) - \ln\left(2\sinh\frac{\beta E}{2}\right)\right] \times \mathcal{D}(\mathbf{k},E)\,dE\,. \tag{37}$$

For an isotropic sample,

$$S_{\rm iso} = k_B\int\left[\frac{\beta E}{2}\coth\left(\frac{\beta E}{2}\right) - \ln\left(2\sinh\frac{\beta E}{2}\right)\right]g(E)\,dE = \frac{1}{3}\,S\,, \tag{38}$$

while for a powder sample,

$$S_{\rm pow} = k_B \int |\epsilon(E)|^2 \left[\frac{\beta E}{2} \coth\left(\frac{\beta E}{2}\right) - \ln\left(2\sinh\frac{\beta E}{2}\right)\right] \times g(E)\, dE\,. \quad (39)$$

The projected partial isochoric specific heat is given by

$$C_{V\hat{k}} = k_B \int \left(\frac{\beta E}{2}\right)^2 \mathrm{csch}^2\left(\frac{\beta E}{2}\right) \mathcal{D}(\mathbf{k},E)\, dE\,. \quad (40)$$

For an isotropic sample,

$$C_{\rm iso} = k_B \int \left(\frac{\beta E}{2}\right)^2 \mathrm{csch}^2\left(\frac{\beta E}{2}\right) g(E)\, dE = \frac{1}{3} C_V\,, \quad (41)$$

while for a powder sample,

$$C_{\rm pow} = k_B \int |\epsilon(E)|^2 \left(\frac{\beta E}{2}\right)^2 \mathrm{csch}^2\left(\frac{\beta E}{2}\right) g(E)\, dE\,. \quad (42)$$

Force constant is a useful concept to describe bonding in the lattice. There are several ways to define force constants emphasizing different aspects of lattice bonds. Each normal mode has an equivalent force constant that is proportional to its frequency squared. One can thus define an average of all equivalent force constants as the mean force constant along photon direction,

$$K_{\hat{k}} = \int \tilde{m} \left(\frac{E}{\hbar}\right)^2 \mathcal{D}(\mathbf{k},E)\, dE = \frac{\tilde{m}}{\hbar^2} g_2(\mathbf{k}). \quad (43)$$

For an isotropic sample,

$$K_{\rm iso} = \int \tilde{m} \left(\frac{E}{\hbar}\right)^2 g(E)\, dE = K, \quad (44)$$

and for a powder sample,

$$K_{\rm pow} = \int |\epsilon(E)|^2\, \tilde{m} \left(\frac{E}{\hbar}\right)^2 g(E)\, dE. \quad (45)$$

It is independent of temperature and weighted more by the high-frequency part of a phonon spectrum. Later, we will see that it is the second derivative of the lattice potential in a quasiharmonic approximation. This is also called stiffness in mechanics. We give two more definitions of force constants below.

In an analogy to a simple harmonic oscillator, we can define a characteristic force constant

$$K^c_{\hat{k}} \equiv \frac{2\, T_{\hat{k}}}{\langle z^2\rangle} = \frac{\tilde{m}}{\hbar^2} \frac{\tilde{g}_1}{\tilde{g}_{-1}}\,, \quad (46)$$

with the result expressed in terms of ppDOS moments. Unlike $K_{\hat{k}}$, it is temperature dependent. Also we see that the low-energy part has more weight in its value.

Recently, an effective force constant named resilience was introduced in the study of protein dynamics.[29] It is proportional to the inverse of the temperature rate of change of mean square displacement. In the context of NRIXS, we can define its projected partial contribution from resonant nucleus sublattice as

$$K'_{\hat{k}} \equiv \frac{k_B}{d\langle z^2\rangle/dT}\,. \quad (47)$$

Its high-temperature approximation was studied and identified to be proportional to the inverse of the second inverse moment of DOS.[30] To apply this concept to a sample often measured at low temperatures, we derive $d\langle z^2\rangle/dT$ in the quasiharmonic model, by taking the derivative with respect to T in Eq. (29):

$$\frac{d\langle z^2\rangle}{dT} = \frac{\hbar^2}{\tilde{m} k_B T^2} \int \frac{e^{\beta E}}{(e^{\beta E}-1)^2} \mathcal{D}(\mathbf{k},E)\, dE\,. \quad (48)$$

It is also temperature dependent, in contrast to the mean force constant as in Eq. (43). At high temperatures, where βE is sufficiently small over the whole range of phonon spectrum, one can use the following limit:

$$\frac{d\langle z^2\rangle}{dT} \simeq \frac{\hbar^2 k_B}{\tilde{m}} \int \frac{1}{E^2} \mathcal{D}(\mathbf{k},E)\, dE = \frac{\hbar^2 k_B}{\tilde{m}} g_{-2}(\mathbf{k})\,. \quad (49)$$

The temperature rate of change of mean square displacement in Eq. (48) can also be used to characterize the decrease of the Lamb-Mössbauer factor with rising temperatures. It is then related to a critical temperature.[31] One can expand the mean-square displacement near a fixed temperature T_0:

$$\langle z^2(T)\rangle \approx \langle z^2\rangle|_{T_0} + \frac{d\langle z^2\rangle}{dT}\,\Delta T\,, \quad (50)$$

so we have

$$f(\mathbf{k},T) = e^{-k^2\langle z^2(T)\rangle} = f(\mathbf{k},T_0)\, e^{-(T-T_0)/T_c}\,, \quad (51)$$

where the critical temperature is defined as

$$\frac{1}{T_c} \equiv k^2 \frac{d\langle z^2\rangle}{dT}\,. \quad (52)$$

IV. MOMENT RELATIONS

In the previous sections, we have described both the NRIXS spectrum $S(\mathbf{k},E)$ and the projected partial phonon DOS $\mathcal{D}(\mathbf{k},E)$, and their own sets of moments. Mathematically, these two functions are equivalent in a quasiharmonic lattice model, in the sense that at any given temperature, one can be derived from the other. As a result, one may expect that there exist relationships between the two sets of moments, which we will recover in the following.

Now let us calculate the central moments of $S(\mathbf{k},E)$, as defined in Eq. (4), in the quasiharmonic approximation, which means using the intermediate scattering function, Eq. (B3), and its harmonic expression Eq. (B12). Following the calculations in Appendix C, we have

$$R_l(\mathbf{k}) = (-i\hbar)^l\, f(\mathbf{k}) \frac{d^l e^{\tilde{M}(\mathbf{k},t)}}{dt^l}\bigg|_{t=0}\,, \quad (53)$$

where

$$\tilde{M}(\mathbf{k},t) = M(\mathbf{k},t) - \frac{i}{\hbar} E_R t, \quad (54)$$

whose derivatives at $t=0$ can be expressed in moments of ppDOS, as shown in Eq. (C7). Carrying out the derivatives in Eq. (53) allows us to express $R_l(\mathbf{k})$ in terms of DOS moments. Here, we list a few:

$$R_1(\mathbf{k}) = 0, \quad (55)$$

$$R_2(\mathbf{k}) = 2\, E_R\, \tilde{g}_1(\mathbf{k}), \quad (56)$$

$$R_3(\mathbf{k}) = E_R\, g_2(\mathbf{k}), \tag{57}$$

$$R_4(\mathbf{k}) = 12\, E_R^2\, \tilde{g}_1^2(\mathbf{k}) + 2\, E_R\, \tilde{g}_3(\mathbf{k}), \tag{58}$$

$$R_5(\mathbf{k}) = 20\, E_R^2\, \tilde{g}_1(\mathbf{k})\, g_2(\mathbf{k}) + E_R\, g_4(\mathbf{k}), \tag{59}$$

$$R_6(\mathbf{k}) = 120\, E_R^3\, \tilde{g}_1^3(\mathbf{k}) + 60\, E_R^2\, \tilde{g}_1(\mathbf{k})\, \tilde{g}_3(\mathbf{k}) + 10\, E_R^2\, g_2^2(\mathbf{k}) + 2\, E_R\, \tilde{g}_5(\mathbf{k}), \tag{60}$$

$$R_7(\mathbf{k}) = 420\, E_R^3\, \tilde{g}_1^2(\mathbf{k})\, g_2(\mathbf{k}) + 42\, E_R^2\, \tilde{g}_1(\mathbf{k})\, g_4(\mathbf{k}) + 70\, E_R^2\, g_2(\mathbf{k})\, \tilde{g}_3(\mathbf{k}) + E_R\, g_6(\mathbf{k}). \tag{61}$$

It is interesting to note that all the odd-ordered moments of ppDOS involved are those thermalized moments defined in Eq. (28), while all the even-ordered ones are the regular ones as in Eq. (27). It also reveals that, in a quasiharmonic model, even though $S(\mathbf{k},E)$ is a function of temperature, its first and third moments are not. One of the above relations, Eq. (57), connects Eqs. (10) and (43) and provides an interpretation for the mean force constant $K_{\hat{\mathbf{k}}}$ along the photon direction as a weighted average of all force constants of each normal mode. Approximations of the above set of relations were derived in a previous study[7] by expanding the thermalized moments in powers of temperature thus using only the regular moments of ppDOS.

These relations can be employed to check the consistency of the derived phonon DOS to an NRIXS spectrum. Another utility is to estimate thermodynamic properties from an NRIXS measurement. By inverting the above set of equations, one can calculate DOS moments in terms of R_l, as given explicitly in Appendix C. Many thermodynamic functions or their approximations are expressed in DOS moments. Thus one can make estimations based on the moments of an NRIXS spectrum. A recent study of iron isotope fractionation uses this approach to calculate β factors, the reduced partition function ratios, from NRIXS measurements.[7] This may have advantages over the calculations based on a derived ppDOS, not only because of less data processing, but more importantly, by taking advantage of the fact that odd-ordered moments of $S(\mathbf{k},E)$ are much less sensitive to any constant background that may be present in a measurement. In a previous study, the first moment of $S(E)$ and its relation to the integral of DOS were discussed in the context of normalizing an NRIXS spectrum.[24]

V. MULTIPLE SITES

Now, let us relax the assumption made earlier that there is only one equivalent site in the sample under study. Suppose there are n nonequivalent sites. We can then group the equivalent site terms together and rewrite the right-hand side of Eq. (B4) into sums of nonequivalent sites:

$$F(\mathbf{k},t) = \sum_j^n p_j\, f_j(\mathbf{k})\, e^{M_{jj}(\mathbf{k},t)} = \sum_j^n p_j F^{(j)}(\mathbf{k},t), \tag{62}$$

where $p_j = \tilde{N}_j/\tilde{N}$ is the fraction of equivalent sites of type j among all the sites occupied by resonant nuclei with $\sum p_j = 1$, $f_j(\mathbf{k}) = e^{-W_j(\mathbf{k})}$ is the directional Lamb-Mössbauer factor of that site, and the site-specific intermediate scattering function

$$F^{(j)}(\mathbf{k},t) = f_j(\mathbf{k})\, e^{M_{jj}(\mathbf{k},t)}. \tag{63}$$

If we also define site-specific phonon excitation probability density functions and site-specific projected partial phonon density of states,

$$S^{(j)}(\mathbf{k},E) = \frac{1}{2\pi\hbar}\int F^{(j)}(\mathbf{k},t)\, e^{-iEt/\hbar}\, dt \tag{64}$$

$$= \sum_{n=0} \frac{f_j(\mathbf{k})}{2\pi\hbar}\int \frac{M_{jj}^n(\mathbf{k},t)}{n!}\, e^{-iEt/\hbar}\, dt = \sum_{n=0} S_n^{(j)}(\mathbf{k},E), \tag{65}$$

$$\mathcal{D}^{(j)}(\mathbf{k},E) = \frac{1}{N}\sum_{s=1}^{3N} \left(\hat{\mathbf{k}}\cdot\epsilon_s^j\right)^2 \delta\left(E - E_s^{(j)}\right), \tag{66}$$

then it can be shown that all the relationships derived above for a single site still hold per site; all we need to do is to attach a site label j. Since moments are linear functionals of a distribution function, we can assemble total moments from site specific ones rather straight-forwardly. However, we point out that even though the relations in Eqs. (55)–(61) in Sec. IV hold for each individual site, the corresponding ones for the whole measured spectrum are more complicated due to the nonlinear nature of these relations, except for the first three which are linear.

Furthermore, in cases of multiple nonequivalent sites, there is a caveat that neither the site-specific ppDOS nor the site-specific f factors can be derived from an NRIXS measurement alone. In general, one cannot separate out individual site contributions to $S(\mathbf{k},E)$.[26] Only in certain limiting situations, e.g., when each site-specific f factor is sufficiently high so that multiple phonon contributions may be ignored, or in cases of amorphous materials where resonant nuclei are situated in almost identical local environments, can the problem then be resolved in approximations.

This points to the importance of the simulation of $S(\mathbf{k},E)$ from a model phonon DOS in NRIXS studies. The simulations can be compared to measurements as a way to check the models and provide insights and understanding for the improvement of the lattice dynamic models.

VI. THERMODYNAMICS OF THREE MINERALS

In a recent study of iron isotope fractionation concerning the redox conditions of rocks on Earth and possibly Mars, NRIXS spectra of goethite, potassium-jarosite, and hydronium-jarosite were measured at the nuclear resonant scattering beamline at the Advanced Photon Source.[7] Here, we present the various atomic dynamics and thermodynamic quantities of these minerals derived from these measurements.

Before showing the results, we want to discuss a particular issue in NRIXS method, which concerns the energy range taken in an experiment. In theory, a phonon excitation spectrum $S(\mathbf{k},E)$ extends to a very large energy range, especially at room temperature or higher. However, towards both ends of a spectrum, where it is dominated by multiphonon contributions, the intensity of the spectrum is exceedingly small as energy increases. In practice, the range taken must be

TABLE II. Quantities derived from an NRIXS measurement of goethite FeO(OH), at the sample temperature of 301 K.

	raw $S(\mathbf{k},E)$	simulated $S(\mathbf{k},E)$	$\mathcal{D}(\mathbf{k},E)$
Lamb-Mössbauer factor, f	0.780 ± 0.005	0.782	0.782
Mean square displacement, $\langle z^2\rangle$ (Å^2)	0.00466 ± 0.00012	0.00461	0.00461
Mean kinetic energy, $T_{\hat{k}}$ (meV)	15.58 ± 0.13	15.13	15.15
Mean force constant, $K_{\hat{k}}$ (N/m)	305.8 ± 9.4	320.7	322.7
Characteristic force constant, $K^c_{\hat{k}}$ (N/m)	107.1 ± 2.9	105.1	105.2
Effective force constant, $K'_{\hat{k}}$ (N/m)			100.3
$d\langle z^2\rangle/dT$ (Å^2/K)			0.000014
Critical temperature, T_c (K)			1362
$d\langle z^2\rangle/dT$ (Å^2/K), high-T limit			0.000015
Critical temperature, T_c (K), high-T limit			1286
Helmholtz free energy, $F_{\hat{k}}$ (meV)			5.12
Internal energy, $U_{\hat{k}}$ (meV)			30.3
Vibrational entropy, $S_{\hat{k}}$ (k_B)			0.971
Phonon specific heat, $C_{\hat{k}}$ (k_B)			0.856
Isotope fractionation factor, $ln\beta$ ($\Delta m/m$)	0.302 ± 0.015	0.250	0.252

limited due to this vanishing scattering intensity and available time for an experiment. Nonetheless, the part of the spectrum not included in the energy range where the data are taken may make noticeable contributions to the higher moments. And indeed, this does manifest itself in the moments extracted. A common observation is that often there are discrepancies in the moment relations (56) and (57), as can be seen by comparing the "raw $S(\mathbf{k},E)$" and "$\mathcal{D}(\mathbf{k},E)$" columns in the data Tables II–IV. One of the possible contributions to this discrepancy could be the limited energy range over which the data are taken. However, one should keep in mind that the results from $\mathcal{D}(\mathbf{k},E)$ are highly sensitive to the background subtraction in data processing.

To alleviate this problem, one may assume that the derived ppDOS is a mathematical model for $S(\mathbf{k},E)$, and then use the corresponding simulated function to calculate the moments. These "simulated $S(\mathbf{k},E)$" values are also listed in the data tables. The agreement between these and the values in the "$\mathcal{D}(\mathbf{k},E)$" column is guaranteed because they both are derived from the same function, the ppDOS. We should emphasize that the "simulated" values are our best estimates based on the assumption of a quasiharmonic lattice model and that all the phonon modes are within the energy range being used. In cases where appreciable anharmonic effects are suspected, one would want to measure the spectra in an energy range as large as possible. We should also keep in mind that in some cases of multiple nonequivalent sites ppDOS cannot be derived from measurement, as discussed in Sec. V.

The data taken of the three minerals are shown in Fig. 1. The experimental details are described in Ref. 7. The derived ppDOS are plotted in Fig. 2. In the following Tables II–IV, we list the atomic dynamics and thermodynamic quantities derived from the NRIXS measurements. The isotope fractionation factors are calculated from mean kinetic energy.[6] In the tables, error estimates are not given for those values calculated from ppDOS because the error estimates of ppDOS are not

TABLE III. Quantities derived from an NRIXS measurement of hydronium-jarosite $(H_3O)Fe_3(SO_4)_2(OH)_6$, at the sample temperature of 301 K.

	raw $S(\mathbf{k},E)$	simulated $S(\mathbf{k},E)$	$\mathcal{D}(\mathbf{k},E)$
Lamb-Mössbauer factor, f	0.652 ± 0.004	0.667	0.667
Mean square displacement, $\langle z^2\rangle$ (Å^2)	0.00802 ± 0.00013	0.00760	0.00760
Mean kinetic energy, $T_{\hat{k}}$ (meV)	16.23 ± 0.12	15.16	15.17
Mean force constant, $K_{\hat{k}}$ (N/m)	307.3 ± 9.0	327.1	329.5
Characteristic force constant, $K^c_{\hat{k}}$ (N/m)	64.9 ± 1.1	63.9	64.0
Effective force constant, $K'_{\hat{k}}$ (N/m)			58.8
$d\langle z^2\rangle/dT$ (Å^2/K)			0.000023
Critical temperature, T_c (K)			798
$d\langle z^2\rangle/dT$ (Å^2/K), high-T limit			0.000024
Critical temperature, T_c (K), high-T limit			766
Helmholtz free energy, $F_{\hat{k}}$ (meV)			2.88
Internal energy, $U_{\hat{k}}$ (meV)			30.3
Vibrational entropy, $S_{\hat{k}}$ (k_B)			1.06
Phonon specific heat, $C_{\hat{k}}$ (k_B)			0.857
Isotope fractionation factor, $ln\beta$ ($\Delta m/m$)	0.378 ± 0.014	0.253	0.255

TABLE IV. Quantities derived from an NRIXS measurement of potassium-jarosite $KFe_3(SO_4)_2(OH)_6$, at the sample temperature of 301 K.

	raw $S(\mathbf{k},E)$	simulated $S(\mathbf{k},E)$	$\mathcal{D}(\mathbf{k},E)$
Lamb-Mössbauer factor, f	0.692 ± 0.003	0.703	0.703
Mean square displacement, $\langle z^2\rangle$ (Å^2)	0.00690 ± 0.00008	0.00660	0.00660
Mean kinetic energy, $T_{\hat{k}}$ (meV)	15.48 ± 0.08	15.10	15.11
Mean force constant, $K_{\hat{k}}$ (N/m)	264.8 ± 5.7	315.6	317.2
Characteristic force constant, $K^c_{\hat{k}}$ (N/m)	71.8 ± 1.0	73.4	73.4
Effective force constant, $K'_{\hat{k}}$ (N/m)			68.2
$d\langle z^2\rangle/dT$ (Å^2/K)			0.000020
Critical temperature, T_c (K)			926
$d\langle z^2\rangle/dT$ (Å^2/K), high-T limit			0.000021
Critical temperature, T_c (K), high-T limit			886
Helmholtz free energy, $F_{\hat{k}}$ (meV)			3.38
Internal energy, $U_{\hat{k}}$ (meV)			30.2
Vibrational entropy, $S_{\hat{k}}$ (k_B)			1.03
Phonon specific heat, $C_{\hat{k}}$ (k_B)			0.859
Isotope fractionation factor, $ln\beta$ ($\Delta m/m$)	0.290 ± 0.010	0.246	0.248

independent, and it is very cumbersome to propagate them from the measured spectrum. The error estimates from $S(\mathbf{k},E)$, whenever available, can be used as very good proxies.

The values presented here are in good agreement with those published previously,[7] especially those derived from the raw $S(\mathbf{k},E)$. This is a different analysis of the data. Here, we fix the sample temperatures and the constant backgrounds according to an estimate based on measurements of background before the data was taken. Uncertainties in the background estimate could significantly change the results derived from simulated $S(\mathbf{k},E)$ and $\mathcal{D}(\mathbf{k},E)$. This is an issue to be carefully studied and also requires proper care to be taken during an experiment. In Table IV for K-jarosite, the results for mean force constant show very large discrepancies. A close inspection reveals that the raw S(E) has excess intensities on the phonon annihilation side comparing to the simulated S(E) calculated from ppDOS. The excess is still present even if one would raise the sample temperature in data analysis. The significant discrepancy requires further study.

VII. ERROR ESTIMATIONS

We now try to answer the question of how accurate and precise the moments derived from an NRIXS measurement are? A few sources of possible errors are considered and discussed. The effect of a finite energy bandwidth of the x-ray beam used in an experiment is considered in Sec. II, where corrections are given using the moments of the finite resolution function.

In the previous section, we mention the errors caused by the background counts in a measured spectrum. Obviously, a changing background is almost impossible to deal with after the fact. Care should be taken to minimize the level and variability of contributing backgrounds. A good practice is to measure the background before a measurement starts and monitor it from time to time during the measurements in between scans. A correction to R_l due to a constant background

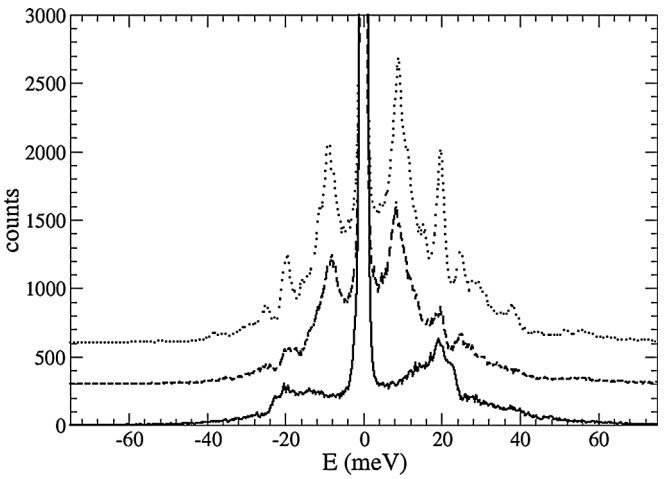

FIG. 1. The measured NRIXS spectra of goethite (the solid line), hydronium-jarosite (the dashed line), and potassium-jarosite (the dotted line). Here, it only shows data in an energy range of ±75 meV, while the actual data collection range was −120 to +130 meV.

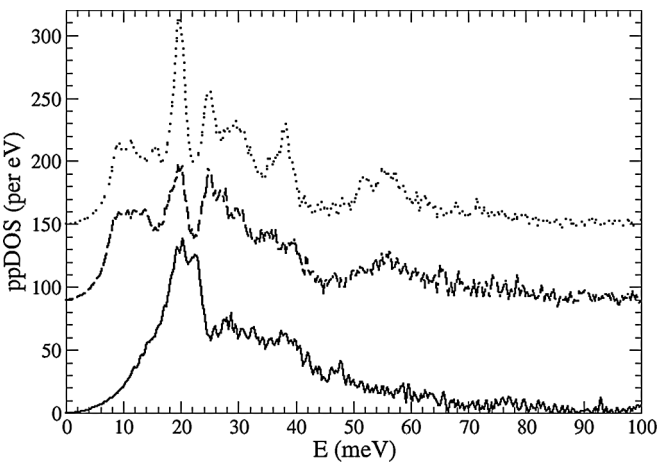

FIG. 2. The ppDOS of goethite (the solid line), hydronium-jarosite (the dashed line), and potassium-jarosite (the dotted line). Here, it only shows data in an energy range up to 100 meV.

b can be estimated as

$$\frac{b/\Delta}{l+1}\left[(E_{\max}-E_R)^{l+1}-(E_{\min}-E_R)^{l+1}\right], \tag{67}$$

where $(E_{\min}, E_{\max})$ is the energy range where data is taken and Δ is the step size. The two terms in the correction tend to cancel each other for odd moments. If the energy range is entered around E_R, the cancellation is complete and there is no correction from a constant background.

The issue of limited energy range has been discussed also. It is advisable to take data over the maximum energy range before the background count rate is reached in cases of anharmonicity. With a valid quasiharmonic approximation, the simulated $S(E)$ can be used to make up for a truncated range.

Due to counting statistics, $S(\mathbf{k}, E)$ has uncertainties at each spectral point, $S_i \pm \sigma_{S_i}$. Assuming Poisson distributions,

$$\sigma_{S_i}^2 = a\, S_i\,, \tag{68}$$

where a is the normalization factor from the measured spectrum to $S(\mathbf{k}, E)$. A smaller value of a indicates better statistics. Using a discrete formulation of the central moments,

$$R_l = \sum (E_i - E_R)^l\, S_i\, \Delta\,, \tag{69}$$

we have

$$\sigma_{R_l}^2 = a\, \Delta\, R_{2l}\,. \tag{70}$$

The energies of a spectrum are determined by tuning a high-resolution monochromator.[32] Due to temperature variations and finite motion precision, there are variations in the energies, which we will represent using a single number σ_E that is independent of the energy. Again, using the discrete formulation of the central moments, we have

$$\sigma_{R_l}^2 = l^2\Delta^2\sigma_E^2 \sum [S_i(E_i - E_R)^{l-1}]^2\,. \tag{71}$$

Another possible source of uncertainties of energy is scaling, stemming from the above mentioned fact that the energies are determined by the motions of high-resolution monochromator crystals. Scaling is the first-order approximation of this possible energy-dependent variations in energy. Assuming a possible scaling error in energies, $E \to (1+\delta)E$, we can calculate that the resulting relative error in R_l is

$$\frac{\Delta R_l}{R_l} = \sum_{m=0}^{l} \frac{R_{l-m}}{R_l} E_R^m \sum_{k=m}^{l} C_l^k C_k^m \delta^k - 1\,. \tag{72}$$

To the first order of δ,

$$\frac{\Delta R_l}{R_l} \simeq l\left(1 + \frac{R_{l-1}}{R_l} E_R\right)\delta \simeq l\,\delta\,. \tag{73}$$

We plot error estimates of moments derived from an NRIXS measurement of a goethite sample at room temperature in Fig. 3. The values are from the three possible sources estimated above, those from counting statistics, energy variations, and an energy scaling error. The experiment done has a good counting rate resulting in reasonable statistical error estimates for the moments, particularly the second and third moments. We use very conservative estimates of energy variation of $\sigma_E = 0.1$ meV and an energy scaling uncertainty of $\delta = 1\%$. We observe that while small energy variations have negligible effect on the moments, they are very sensitive to energy scaling. Thus accurate energy scale calibration is very important and should be done carefully.

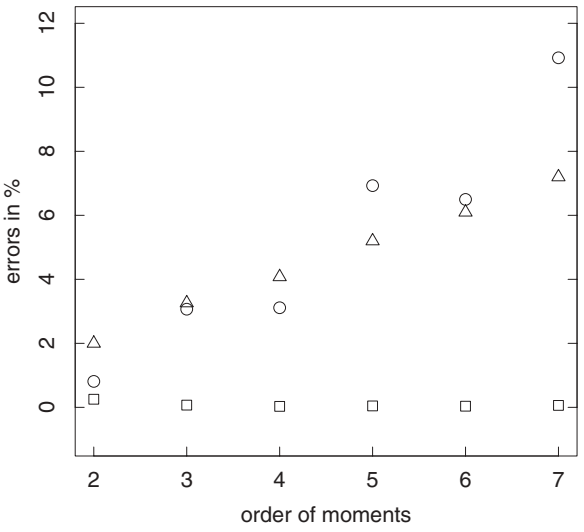

FIG. 3. The relative error estimates of the moments due to counting statistics (circles), energy variations (squares), and energy scaling error (triangles). The estimates are based on the data taken for a sample of goethite.

VIII. SUMMARY

We have studied the moments of an NRIXS spectrum and the derived ppDOS. Explicit relations between the two sets of moments are given. Dynamical and thermodynamic properties calculated from the spectrum are explained, and their directional nature is emphasized. Three force-constant-like quantities are introduced to help characterize bondings in a lattice. The third and fourth moments of an NRIXS spectrum are calculated beyond the quasiharmonic approximation. This reveals the possible utility of this method to help constrain and improve the quartic anharmonic term of lattice potential models. Issues related to the calculation of moments are discussed, including the effect of resolution function, energy range over which the spectrum is taken, and multiple nonequivalent sites. Uncertainties of the moments derived from a measured spectrum are estimated for the possible causes due to statistical quality, energy variations, and energy scaling error. We have explored the rich content of the moments in NRIXS and their potential applications in lattice dynamic and thermodynamic studies of materials and hope that the details contained here may help researchers evaluate and interpret their results from NRIXS experiments.

ACKNOWLEDGMENTS

M.Y.H. thanks Harry Lipkin for inspiration and detailed discussions. He also appreciates helpful discussions with J. Timothy Sage, Wolfgang Sturhahn, Aleksandr I. Chumakov, Brent Fultz, Raphael Hermann, and referees of the manuscript whose constructive criticism helped improve its presentation and clarity. The NRIXS data analysis package PHOENIX[33] was used in this work. We also used the statistical package R[34] and the plotting software GRACE[35] to process and visualize data.

Use of the Advanced Photon Source, an Office of Science User Facility operated for the US Department of Energy (DOE) Office of Science by Argonne National Laboratory, was supported by the US DOE under Contract No. DE-AC02-06CH11357. N.D. is partially supported by grants NASA NNX09AG59G and NSF EAR Petrology and Geochemistry (EAR-1144429).

APPENDIX A: CALCULATION OF CENTRAL MOMENTS OF S(E)

Following the formalism laid out previously by Lipkin,[15] we write $S(\mathbf{k},E)$ and $R_l(\mathbf{k})$ in terms of a lattice Hamiltonian and phonon transition matrix elements. In the weak scattering limit, we sum over all nuclei the transition matrix elements due to a sudden momentum transfer,

$$S(\mathbf{k},E) = \frac{1}{\tilde{N}} \sum_{\nu} \sum_{i,f} g_i |\langle f|e^{i\mathbf{k}\mathbf{r}_\nu}|i\rangle|^2 \delta(E + E_i - E_f), \quad \text{(A1)}$$

where g_i is the statistical distribution of initial lattice state $|i\rangle$ at a finite temperature. For all equivalent sites,

$$S(\mathbf{k},E) = \sum_{i,f} g_i |\langle f|e^{i\mathbf{k}\mathbf{r}}|i\rangle|^2 \delta(E + E_i - E_f). \quad \text{(A2)}$$

The moments as defined in Eq. (4) are then

$$R_l(\mathbf{k}) = \sum_{i,f} g_i \, (E_f - E_i - E_R)^l |\langle f|e^{i\mathbf{k}\mathbf{r}}|i\rangle|^2 \quad \text{(A3)}$$

$$= \sum_{i} g_i \, \langle i|e^{-i\mathbf{k}\mathbf{r}}(H - E_i - E_R)^l e^{i\mathbf{k}\mathbf{r}}|i\rangle \quad \text{(A4)}$$

$$= \sum_{i} g_i \, \langle i| \left(H - E_i - \frac{\hbar\mathbf{k}}{\tilde{m}}\mathbf{p}\right)^l |i\rangle, \quad \text{(A5)}$$

where the following operator identity was used:

$$e^{-i\mathbf{k}\mathbf{r}} \, H \, e^{i\mathbf{k}\mathbf{r}} = H - \frac{\hbar\mathbf{k}}{\tilde{m}}\mathbf{p} + E_R. \quad \text{(A6)}$$

Let us rewrite $\mathbf{k}\mathbf{p} = kp_z$ and the operator in Eq. (A5) as

$$A = H - E_i - \frac{\hbar\mathbf{k}}{\tilde{m}}\mathbf{p} = T - \frac{\hbar k}{\tilde{m}}p_z - E_i + V \quad \text{(A7)}$$

with

$$T = \sum_{\mu} \frac{p_\mu^2}{2m_\mu}, \quad \text{(A8)}$$

$$V = \frac{1}{2}\sum_{\mu\mu'} V(\mathbf{r}_\mu, \mathbf{r}_{\mu'}). \quad \text{(A9)}$$

We have the following identities:

$$H|i\rangle = E_i|i\rangle, \quad \text{(A10)}$$

$$A|i\rangle = -\frac{\hbar k}{\tilde{m}}p_z|i\rangle, \quad \text{(A11)}$$

$$\langle i|p_z^{2n+1}|i\rangle = 0, \quad \text{(A12)}$$

$$\langle i|\frac{\partial V}{\partial z}|i\rangle = 0. \quad \text{(A13)}$$

Here p_z is an operator, as the lattice states are not eigenstates of the momentum operator. Equation (A12) reflects time-reversal invariance of the interaction, while Eq. (A13) demonstrates the fact that the system is in equilibrium.

We also have the following commutators, which are used in derivations later:

$$[p_z, H] = [p_z, V] = -i\hbar\frac{\partial V}{\partial z}, \quad \text{(A14)}$$

$$\big[p_z,[p_z,V]\big] = -\hbar^2\frac{\partial^2 V}{\partial z^2}, \quad \text{(A15)}$$

$$\big[p_z^2,[p_z,V]\big] = -\hbar^2\left(p_z\frac{\partial^2 V}{\partial z^2} + \frac{\partial^2 V}{\partial z^2}p_z\right). \quad \text{(A16)}$$

The equilibrium condition (A13) is implied in the Hamiltonian. From the following two identities:

$$\langle i|p_z A|i\rangle = -\frac{\hbar k}{\tilde{m}}\langle i|p_z^2|i\rangle, \quad \text{(A17)}$$

$$\langle i|Ap_z|i\rangle = -\frac{\hbar k}{\tilde{m}}\langle i|p_z^2|i\rangle, \quad \text{(A18)}$$

we have

$$-i\hbar\langle i|\frac{\partial V}{\partial z}|i\rangle = \langle i|\,[p_z, A]\,|i\rangle = 0. \quad \text{(A19)}$$

However, the off-diagonal elements are not zero. Since

$$\langle f|p_z A|i\rangle = -\frac{\hbar k}{\tilde{m}}\langle f|p_z^2|i\rangle, \quad \text{(A20)}$$

$$\langle f|Ap_z|i\rangle = \langle f|\left(E_f - E_i - \frac{\hbar k}{\tilde{m}}p_z\right)p_z|i\rangle, \quad \text{(A21)}$$

we have

$$-i\hbar\langle f|\frac{\partial V}{\partial z}|i\rangle = \langle f|\,[p_z, A]\,|i\rangle = (E_f - E_i)\langle f|p_z|i\rangle. \quad \text{(A22)}$$

For the central moments in Eq. (A5), it follows directly that

$$R_1(\mathbf{k}) = -\frac{\hbar k}{\tilde{m}}\sum_i g_i \, \langle i\,|p_z|\,i\rangle = 0, \quad \text{(A23)}$$

$$R_2(\mathbf{k}) = \sum_i g_i \, \langle i|\left(\frac{\hbar k}{\tilde{m}}p_z\right)^2|i\rangle = 4\,E_R\,T_{\hat{\mathbf{k}}}, \quad \text{(A24)}$$

and

$$R_l(\mathbf{k}) = \frac{2E_R}{\tilde{m}}\sum_i g_i \, \langle i|\, p_z\, A^{l-2}\, p_z\,|i\rangle \quad \text{(A25)}$$

for $l > 2$.

For the third moment, we have the following operator identity:

$$p_z A\, p_z = p_z^2 A - p_z[p_z, A] = [p_z, A]p_z + Ap_z^2$$
$$= \tfrac{1}{2}\left(p_z^2 A + Ap_z^2 - \big[p_z,[p_z,A]\big]\right), \quad \text{(A26)}$$

and

$$R_3(\mathbf{k}) = \frac{2E_R}{\tilde{m}}\sum_i g_i \, \langle i|\frac{1}{2}\left(-\big[p_z,[p_z,A]\big] + p_z^2 A + Ap_z^2\right)|i\rangle \quad \text{(A27)}$$

$$= \frac{2E_R}{\tilde{m}}\sum_i g_i \, \langle i|\frac{\hbar^2}{2}\frac{\partial^2 V}{\partial z^2}|i\rangle - \frac{\hbar^3 k^3}{\tilde{m}^3}\sum_i g_i \, \langle i|\, p_z^3|i\rangle \quad \text{(A28)}$$

$$= \frac{\hbar^2 E_R}{\tilde{m}}\sum_i g_i \, \langle i|\,\frac{\partial^2 V}{\partial z^2}|i\rangle. \quad \text{(A29)}$$

For the fourth moment,

$$p_z\,A^2\,p_z = ([p_z,A]+Ap_z)(-[p_z,A]+p_zA) = -([p_z,A])^2 - Ap_z[p_z,A]+[p_z,A]p_zA + Ap_z^2A, \tag{A30}$$

and

$$\begin{aligned} R_4(\mathbf{k}) &= \frac{2E_R}{\tilde{m}}\sum_i g_i\,\langle i|\,-([p_z,A])^2 - Ap_z[p_z,A] \\ &\quad +[p_z,A]p_zA + Ap_z^2A|i\rangle \\ &= \frac{2E_R}{\tilde{m}}\sum_i g_i\left\{\hbar^2\langle i|\left(\frac{\partial V}{\partial z}\right)^2|i\rangle\right. \\ &\quad \left. +\frac{\hbar k}{\tilde{m}}\langle i|\left[p_z^2,[p_z,A]\right]|i\rangle + \frac{\hbar^2k^2}{\tilde{m}^2}\langle i|p_z^4|i\rangle\right\} \\ &= \frac{2E_R}{\tilde{m}}\left\{\left\langle\hbar^2\left(\frac{\partial V}{\partial z}\right)^2\right\rangle + \frac{2E_R}{\tilde{m}}\langle p_z^4\rangle - \frac{\hbar^2E_0}{\tilde{m}c}\left\langle p_z\frac{\partial^2V}{\partial z^2}\right.\right. \\ &\quad \left.\left. +\frac{\partial^2V}{\partial z^2}\,p_z\right\rangle\right\}. \end{aligned} \tag{A31}$$

APPENDIX B: PROJECTED PARTIAL PHONON DOS

Let us introduce an intermediate scattering function

$$F(\mathbf{k},t) = \int d\mathbf{r}\,e^{i\mathbf{kr}}G_a(\mathbf{r},t) \tag{B1}$$

$$= \frac{1}{\tilde{N}}\left\langle\sum_\nu e^{-i\mathbf{k}\mathbf{r}_\nu(0)}e^{i\mathbf{k}\mathbf{r}_\nu(t)}\right\rangle_T, \tag{B2}$$

which is the inverse Fourier transform of the phonon excitation probability density function with respect to E, so that

$$S(\mathbf{k},E) = \frac{1}{2\pi\hbar}\int F(\mathbf{k},t)\,e^{-iEt/\hbar}\,dt\,. \tag{B3}$$

In the quasiharmonic lattice model, we can calculate the intermediate scattering function as defined in Eq. (B2) to be

$$F(\mathbf{k},t) = \frac{1}{\tilde{N}}\sum_\nu^{\tilde{N}} e^{-W_\nu(\mathbf{k})}\,e^{M_{\nu\nu}(\mathbf{k},t)}, \tag{B4}$$

where

$$W_\nu(\mathbf{k}) = \sum_s\left(\frac{\hbar^2}{2\tilde{m}NE_s}\right)\left|\mathbf{k}\cdot\epsilon_s^\nu\right|^2(2n_s+1), \tag{B5}$$

$$M_{\nu\nu}(\mathbf{k},t) = \sum_s\left(\frac{\hbar^2}{2\tilde{m}NE_s}\right)\left|\mathbf{k}\cdot\epsilon_s^\nu\right|^2[(n_s+1)e^{iE_st/\hbar} + n_se^{-iE_st/\hbar}], \tag{B6}$$

and $\tilde{m}$ is the mass of the resonant isotope. We use s to label phonon modes, with energy E_s. The phonon occupation number is given by

$$n_s = \frac{1}{e^{\beta E_s}-1}\,. \tag{B7}$$

The polarization vectors ϵ_s^ν satisfy the orthonormality and closure conditions

$$\frac{1}{N}\sum_\nu^N \epsilon_s^\nu\cdot\epsilon_{s'}^{\nu\dagger} = \delta_{ss'}\,, \tag{B8}$$

$$\frac{1}{3N}\sum_s^{3N}\epsilon_s^\mu\cdot\epsilon_s^{\nu\dagger} = \delta_{\mu\nu}\,. \tag{B9}$$

In Sec. III, thermodynamic quantities are given for isotropic and powder samples. The differences in the expressions for the two cases come from the different behaviours of the polarization vectors in each case. For an isotropic sample,

$$\left|\hat{\mathbf{k}}\cdot\epsilon_s^\nu\right|^2 = \tfrac{1}{3}\,, \tag{B10}$$

while for a powder sample, it has to be averaged over all directions,

$$\frac{1}{4\pi}\int\left|\hat{\mathbf{k}}\cdot\epsilon_s^\nu\right|^2 d\Omega_k = \frac{\left|\epsilon_s^\nu\right|^2}{3}\,. \tag{B11}$$

In a crystal, the polarization vectors are the same at all equivalent sites, so that these sites share the same $W(\mathbf{k})$ and $M(\mathbf{k},t)$. First, let us consider the simple case where all resonant nuclei occupy equivalent sites in a crystal. The intermediate scattering function then takes the form of

$$F(\mathbf{k},t) = e^{-W(\mathbf{k})}\,e^{M(\mathbf{k},t)}\,, \tag{B12}$$

where the functions in Eqs. (B5) and (B6) become identical for all resonant nuclei:

$$W(\mathbf{k}) = \sum_s\left(\frac{\hbar^2}{2\tilde{m}NE_s}\right)(\mathbf{k}\cdot\epsilon_s)^2(2n_s+1)\,, \tag{B13}$$

$$M(\mathbf{k},t) = \sum_s\left(\frac{\hbar^2}{2\tilde{m}NE_s}\right)(\mathbf{k}\cdot\epsilon_s)^2 \times[(n_s+1)e^{iE_st/\hbar}+n_se^{-iE_st/\hbar}]\,. \tag{B14}$$

The first factor on the right-hand side of Eq. (B12) is the directional Lamb-Mössbauer factor

$$f(\mathbf{k}) = e^{-W(\mathbf{k})} = e^{-k^2\langle z^2\rangle}, \tag{B15}$$

where the mean square displacement of the resonant nucleus along the photon direction $\langle z^2\rangle$ is related to the first inverse moment of ppDOS, which is shown in Sec. III.

The expansion of the second exponential in Eq. (B12) into a power series corresponds to single- and multiphonon contributions. Thus we have an expansion of phonon excitation probability density function given as

$$S(\mathbf{k},E) = \sum_{n=0}\frac{f(\mathbf{k})}{2\pi}\int\frac{M^n(\mathbf{k},t)}{n!}\,e^{-iEt/\hbar}\,dt\;=\sum_{n=0}S_n(\mathbf{k},E)\,. \tag{B16}$$

For the zeroth-order term, the integral reduces to a δ function,

$$S_0(\mathbf{k},E) = f(\mathbf{k})\delta(E)\,. \tag{B17}$$

Now we define a projected partial phonon DOS as

$$\mathcal{D}(\mathbf{k},E) = \frac{1}{\tilde{N}}\sum_{\nu=1}^{\tilde{N}}\frac{1}{N}\sum_{s=1}^{3N}\left(\hat{\mathbf{k}}\cdot\epsilon_s^\nu\right)^2\delta(E-E_s)\,, \tag{B18}$$

where $\hat{\mathbf{k}} = \mathbf{k}/k$ is the unit vector of the incident photon direction. In the case of a single identical site, it is simply

$$\mathcal{D}(\mathbf{k},E) = \frac{1}{N}\sum_{s=1}^{3N}(\hat{\mathbf{k}}\cdot\epsilon_s)^2\,\delta(E-E_s)\,. \tag{B19}$$

By going to the continuum limit in Eq. (B14), we can write $M(\mathbf{k},t)$ in terms of the phonon DOS defined above:

$$\begin{aligned} M(\mathbf{k},t) &= \int_0^{+\infty}\frac{E_R}{E}\{[n(E)+1]e^{iEt/\hbar}+n(E)e^{-iEt/\hbar}\} \\ &\quad\times\mathcal{D}(\mathbf{k},E)\,dE \qquad\text{(B20)}\\ &= \int_0^{+\infty}\frac{E_R}{E}\frac{e^{\beta E}}{e^{\beta E}-1}e^{iEt/\hbar}\mathcal{D}(\mathbf{k},E)\,dE \\ &\quad-\int_{-\infty}^{0}\frac{E_R}{E}\frac{1}{e^{-\beta E}-1}e^{iEt/\hbar}\mathcal{D}(\mathbf{k},-E)\,dE \\ &= \int_{-\infty}^{+\infty}\frac{E_R}{E(1-e^{-\beta E})}e^{iEt/\hbar}\tilde{\mathcal{D}}(\mathbf{k},E)\,dE\,, \qquad\text{(B21)}\end{aligned}$$

where $\tilde{\mathcal{D}}(\mathbf{k},E)$ is $\mathcal{D}(\mathbf{k},E)$ extended to negative energies:

$$\tilde{\mathcal{D}}(\mathbf{k},E) = \begin{cases}\mathcal{D}(\mathbf{k},E) & ,\quad E\geqslant 0\\ \mathcal{D}(\mathbf{k},-E), & E<0\end{cases}. \tag{B22}$$

To calculate the first-order one-phonon term, we use Eq. (B21) in carrying out the Fourier transform for $S_1(\mathbf{k},E)$ as defined in Eq. (B16),

$$\begin{aligned} S_1(\mathbf{k},E) &= \frac{f(\mathbf{k})}{2\pi}\int M(\mathbf{k},t)\,e^{-iEt/\hbar}\,dt \qquad\text{(B23)}\\ &= \frac{f(\mathbf{k})E_R}{E(1-e^{-\beta E})}\tilde{\mathcal{D}}(\mathbf{k},E)\,, \qquad\text{(B24)}\end{aligned}$$

which relates the single-phonon excitation probability density to ppDOS. It is the basis for deriving ppDOS from NRIXS measurements, in which the Fourier-Log algorithm is employed to calculate $S_1(\mathbf{k},E)$ from a measured spectrum $S(\mathbf{k},E)$.[22]

In Sec. IV and Appendix C, Eq. (B21) is further exploited to find relations between two sets of moments. We can already see in this equation that it connects $S(\mathbf{k},E)$ in the form of $M(\mathbf{k},t)$ to phonon DOS.

APPENDIX C: CALCULATING MOMENT RELATIONS

To calculate the central moments of $S(\mathbf{k},E)$ in the quasiharmonic approximation, we substitute Eqs. (B3) and (B12) into Eq. (4), acknowledging the fact that the Fourier transform of a power function is a derivative of a δ function,

$$\begin{aligned} R_l(\mathbf{k}) &= \int(E-E_R)^l\,\frac{1}{2\pi\hbar}\int F(\mathbf{k},t)\,e^{-iEt/\hbar}\,dt\,dE \\ &= f(\mathbf{k})\int dt\,e^{M(\mathbf{k},t)}\,\frac{1}{2\pi\hbar}\int(E-E_R)^l e^{-iEt/\hbar}\,dE \\ &= f(\mathbf{k})\int dt\,e^{M(\mathbf{k},t)-iE_Rt/\hbar}\,(i\hbar)^l\,\delta^{(l)}(t) \\ &= f(\mathbf{k})\int(-i\hbar)^l\,\frac{d^l e^{M(\mathbf{k},t)-iE_Rt/\hbar}}{dt^l}\,\delta(t)\,dt \\ &= (-i\hbar)^l\,f(\mathbf{k})\frac{d^l e^{M(\mathbf{k},t)-iE_Rt/\hbar}}{dt^l}\bigg|_{t=0} \\ &= (-i\hbar)^l\,f(\mathbf{k})\frac{d^l e^{\tilde{M}(\mathbf{k},t)}}{dt^l}\bigg|_{t=0}\,, \qquad\text{(C1)}\end{aligned}$$

where

$$\tilde{M}(\mathbf{k},t) = M(\mathbf{k},t) - \frac{i}{\hbar}E_Rt \tag{C2}$$

with derivatives

$$\frac{d\tilde{M}(\mathbf{k},t)}{dt} = \frac{dM(\mathbf{k},t)}{dt} - \frac{i}{\hbar}E_R \tag{C3}$$

and

$$\frac{d^l\tilde{M}(\mathbf{k},t)}{dt^l} = \frac{d^lM(\mathbf{k},t)}{dt^l} \tag{C4}$$

for $l>1$.

Next, we calculate derivatives of $M(\mathbf{k},t)$ from Eq. (B20),

$$\begin{aligned}\frac{d^lM(\mathbf{k},t)}{dt^l} &= \int\frac{E_R}{E}\frac{d^l}{dt^l}\{[n(E)+1]e^{iEt/\hbar}+n(E)e^{-iEt/\hbar}\} \\ &\quad\times\mathcal{D}(\mathbf{k},E)\,dE \\ &= E_R\left(\frac{i}{\hbar}\right)^l\int\{[n(E)+1]e^{iEt/\hbar} \\ &\quad+(-1)^l n(E)e^{-iEt/\hbar}\}E^{l-1}\mathcal{D}(\mathbf{k},E)\,dE\,, \qquad\text{(C5)}\end{aligned}$$

which are then evaluated at $t=0$:

$$\frac{d^lM(\mathbf{k},t)}{dt^l}\bigg|_{t=0} = \begin{cases}E_R\left(\frac{i}{\hbar}\right)^{2n+1}\int E^{2n}\mathcal{D}(\mathbf{k},E)\,dE,\\ E_R\left(\frac{i}{\hbar}\right)^{2n}\int\coth\left(\frac{\beta E}{2}\right)E^{2n-1}\mathcal{D}(\mathbf{k},E)\,dE,\end{cases} \tag{C6}$$

for odd $l=2n+1$ or even $l=2n$. Using the DOS moments defined in Eqs. (27) and (28), we have

$$\frac{d^lM(\mathbf{k},t)}{dt^l}\bigg|_{t=0} = \begin{cases}\left(\frac{i}{\hbar}\right)^{2n+1}E_R\,g_{2n}(\mathbf{k}),\\ 2\left(\frac{i}{\hbar}\right)^{2n}E_R\,\tilde{g}_{2n-1}(\mathbf{k}),\end{cases} \tag{C7}$$

with the help of which, one can calculate R_l in Eq. (C1). The first few are given in Eqs. (55)–(61) in Sec. IV.

Here, we also list the expressions of ppDOS moments in terms of R_l to complete the discussion:

$$\tilde{g}_1(\mathbf{k}) = \frac{R_2(\mathbf{k})}{2E_R}, \tag{C8}$$

$$g_2(\mathbf{k}) = \frac{R_3(\mathbf{k})}{E_R}, \tag{C9}$$

$$\tilde{g}_3(\mathbf{k}) = \frac{R_4(\mathbf{k})-3R_2^2(\mathbf{k})}{2E_R}, \tag{C10}$$

$$g_4(\mathbf{k}) = \frac{R_5(\mathbf{k})-10R_2(\mathbf{k})R_3(\mathbf{k})}{E_R}, \tag{C11}$$

$$\tilde{g}_5(\mathbf{k}) = \frac{R_6(\mathbf{k})+30R_2^3(\mathbf{k})-15R_2(\mathbf{k})R_4(\mathbf{k})-10R_3^2(\mathbf{k})}{2E_R}, \tag{C12}$$

$$g_6(\mathbf{k}) = \frac{R_7(\mathbf{k}) + 210R_2^2(\mathbf{k})R_3(\mathbf{k}) - 21R_2(\mathbf{k})R_5(\mathbf{k}) - 35R_3(\mathbf{k})R_4(\mathbf{k})}{E_R}. \quad \text{(C13)}$$

The even moments were deduced in a previous study using expansions in powers of temperature.[7]

*myhu@aps.anl.gov

[1] R. Röhlsberger, *Nuclear Condensed Matter Physics with Synchrotron Radiation*, Springer Tracts in Modern Physics Vol. 208 (Springer, Heidelberg, 2004).

[2] V. V. Struzhkin, H.-k. Mao, W. L. Mao, R. J. Hemley, W. Sturhahn, E. E. Alp, C. L'Abbe, M. Y. Hu, and D. Errandonea, Hyperfine Interact. **153**, 3 (2004).

[3] W. Sturhahn and J. M. Jackson, GSA Special Paper **421**, 157 (2007).

[4] W. R. Scheidt, S. M. Durbin, and J. T. Sage, J. Inorg. Biochem. **99**, 60 (2005).

[5] V. B. Polyakov, Science **323**, 912 (2009).

[6] V. B. Polyakov and S. D. Mineev, Geochim. Cosmochim. Acta **64**, 849 (2000).

[7] N. Dauphas, M. Roskosz, E. E. Alp, D. C. Golden, C. K. Sio, F. L. H. Tissot, M. Y. Hu, J. Zhao, L. Gao, and R. V. Morris, Geochim. Cosmochim. Acta **94**, 254 (2012).

[8] B. Roldan Cuenya, J. R. Croy, L. K. Ono, A. Naitabdi, H. Heinrich, W. Keune, J. Zhao, W. Sturhahn, E. E. Alp, and M. Hu, Phys. Rev. B **80**, 125412 (2009).

[9] L. Van Hove, Phys. Rev. **95**, 249 (1954).

[10] W. M. Visscher, Annals of Physics **9**, 194 (1960).

[11] K. S. Singwi and A. Sjölander, Phys. Rev. **120**, 1093 (1960).

[12] W. Sturhahn and V. G. Kohn, Hyperfine Interact. **123-124**, 367 (1999).

[13] W. Cochran, Rep. Prog. Phys. **26**, 1 (1963).

[14] E. Burkel, J. Phys.: Condens. Matter **13**, 7627 (2001).

[15] H. J. Lipkin, Phys. Rev. B **52**, 10073 (1995).

[16] H. J. Lipkin, Annals of Physics **18**, 182 (1962).

[17] V. G. Kohn, A. I. Chumakov, and R. Rüffer, Phys. Rev. B **58**, 8437 (1998).

[18] H. J. Lipkin, Hyperfine Interact. **123-124**, 349 (1999).

[19] A. Chumakov and W. Sturhahn, Hyperfine Interact. **123-124**, 781 (1999).

[20] V. Kohn and A. Chumakov, Hyperfine Interact. **125**, 205 (2000).

[21] W. Sturhahn, J. Phys.: Condens. Matter **16**, S497 (2004).

[22] W. Sturhahn, T. S. Toellner, E. E. Alp, X. Zhang, M. Ando, Y. Yoda, S. Kikuta, M. Seto, C. W. Kimball, and B. Dabrowski, Phys. Rev. Lett. **74**, 3832 (1995).

[23] A. I. Chumakov, R. Rüffer, A. Q. R. Baron, H. Grünsteudel, H. F. Grünsteudel, and V. G. Kohn, Phys. Rev. B **56**, 10758 (1997).

[24] V. G. Kohn, A. I. Chumakov, and R. Rüffer, Phys. Rev. B **73**, 094306 (2006).

[25] M. Hu, W. Sturhahn, T. Toellner, P. Hession, J. Sutter, and E. Alp, Nucl. Instrum. Methods Phys. Res. A **428**, 551 (1999).

[26] M. Y. Hu, Ph.D. thesis, Northwestern University, Evanston, Illinois, 1999.

[27] R. Röhlsberger, J. Phys.: Condens. Matter **13**, 7659 (2001).

[28] E. E. Alp, W. Sturhahn, T. S. Toellner, J. Zhao, M. Hu, and D. E. Brown, Hyperfine Interact.**144-145**, 3 (2002).

[29] G. Zaccai, Science **288**, 1604 (2000).

[30] B. M. Leu, Y. Zhang, L. Bu, J. E. Straub, J. Zhao, W. Sturhahn, E. Ercan Alp, and J. Timothy Sage, Biophys. J. **95**, 5874 (2008).

[31] W. Sturhahn (private communication).

[32] T. Toellner, Hyperfine Interact. **125**, 3 (2000).

[33] W. Sturhahn, Hyperfine Interact. **125**, 149 (2000).

[34] R Development Core Team, R: A Language and Environment for Statistical Computing, R Foundation for Statistical Computing, Vienna, Austria (2011), http://www.R-project.org/.

[35] GRACE Development Team, GRACE (2012), http://plasma-gate.weizmann.ac.il/Grace/.